Pak. j. life soc. Sci. (2024), 22(2):13311-13326 E-ISSN: 2221-7630;P-ISSN: 1727-4915

Pakistan Journal of Life and Social Sciences
www.pjlss.edu.pk

https://doi.org/10.57239/PJLSS-2024-22.2.00954

RESEARCH ARTICLE

Thiourea-Modified Porous Activated Carbon for Efficient Adsorption of Lead (II) From Water: Kinetic, Isotherm and Adsorption Studies

Abdullah Saeed AlShahrani[1], Bassem Jamoussi[1], Nagwa T. Elsharawy[2*], Riyadh F. Halawani[3], Abdullatif A. Neamatallah[1]

[1]Department of Environment, Faculty of Environmental Sciences, King Abdulaziz University, Jeddah 21589, Saudi Arabi
[2*]Department of Sport Science & Health, College of Sport Science, University of Jeddah, Jeddah, Saudi Arabia.
[2]Department of Food Hygiene, Faculty of Veterinary Medicine, New Valley University, 72713, Egypt.
[3]Department of Environment, Faculty of Environmental Sciences, King Abdulaziz University, Jeddah 21589, Saudi Arabia.

ARTICLE INFO

Received: Sep .29, 2024

Accepted: Nov 15, 2024

Keywords

Thiourea

Activated carbon

Adsorption

Isotherm

Mechanism

Toxic Pb(II)

***Corresponding Author:**

dr.nagwa2004@yahoo.com

ABSTRACT

This research presents the development of a novel adsorbent, ACDS@Tu, created by chemically modifying activated carbon (AC) derived from date seeds with thiourea (Tu) for the improved removal of Pb(II) ions from water. ACDS@Tu was characterized using FTIR, SEM, BET surface area analysis, and TGA, confirming the structural and functional modifications achieved through thiourea treatment. The surface area and pore volume were measured as 889 m^2/g and 0.158 cm^3/g for ACDS, reduced to 155 m^2/g and 0.03 cm^3/g for ACDS@Tu. ACDS@Tu showed a substantial adsorption capacity of 310.9 mg/g under optimal conditions, aligning with the Langmuir isotherm model and achieving a high adsorption capacity of 503.27 mg/g. Kinetic analysis indicated that the adsorption followed a PSO model. At the same time, thermodynamic studies revealed that the process was favorable, spontaneous, and exothermic—the primary adsorption mechanism involved electrostatic interactions with minimal coordination effects. Overall, ACDS@Tu shows promise as an effective solution for Pb(II) removal from water, offering significant potential for environmental remediation applications.

INTRODUCTION

Water contamination by toxic heavy metals represents a critical global challenge, significantly impacting the environment and public health (Algethami, et al., 2022; Naushad, et al., 2020 and Alqadami et al., 2020 Alqadami et al., 2020[a]). Metals such as chromium (Cr), mercury (Hg), cadmium (Cd), and lead (Pb) are known for their severe toxicity, even in minimal concentrations (Alqadami et al., 2017: Algamdi, et al., 2017; Khan et al., 2019[a] and Saad et al., 2017). Unlike organic contaminants, heavy metals persist in ecosystems without degradation over time, leading to long-lasting environmental impacts (Lee et al., 2022 and Ahamad et al., 2020). Once in aquatic systems, these metals can bioaccumulate in organisms, posing severe risks to marine life and human health

(Alqadami et al., 2020[a]). Lead (Pb(II)), in particular, poses a heightened threat due to its toxicity and tendency to bioaccumulate within food chains (Alqadami et al., 2020[b] and Khanet al., 2019[a]. Industrial activities—mining, dye production, paper manufacturing, metallurgical processing, battery storage, and electroplating—introduce Pb(II) ions into water bodies through wastewater discharges, further amplifying the contamination issue (Alsuhybani et al., 2020). Pb(II) has numerous harmful effects on human health, including central nervous system dysfunction, kidney damage, and brain damage, even at small concentrations. This makes it a severe environmental and public health hazard (Aldawsari et al, 2017). The recommended set limit by the World Health Organization (WHO) for lead in drinking water is 10 µg/L (Maneechakr and Karnjanakom, 2021) emphasizing the need for effective wastewater treatment before distribution (Kariri et al., 2024).

Researchers have developed several treatment techniques to remove toxic heavy metals from wastewater, for example, solvent extraction, electrochemical removal, chemical precipitation, coagulation, floatation, reverse osmosis, and ion exchange adsorption (Zhu, et al., 2016; Wang et al., 2016; Di Palma et al., 2002; Ghasemi, et al., 2014; Matlock et al., 2002; Fu & Wang, 2019; Burke, et al., 2013 and Naushad, 2014). Among the various technologies, adsorption is widely employed for treating wastewater contaminated with Pb(II) ions due to its high effectiveness, simple operation, low cost, and minimal secondary pollution. In contrast, other methods are often more expensive and may produce secondary pollutants (Majdoubi et al., 2023; Khan et al., 2023; Melhi et al., 2022; Algethami et al., 2024).

Among various adsorbents, activated carbon has garnered significant attention and widespread use for heavy metals and dye removal from the water environment. Among various adsorbents, activated carbon has garnered considerable attention and widespread use for heavy metals and dye removal from the water environment because of its unique properties, including a wide variety of functional groups, a large surface area, and an excellent porous structure (Naushad, et al., 2020; Aldawsari et al., 2021). Several studies for Pb(II) removal have been carried out using activated carbon derived from waste biomass such as pine cone (Momčilović et al., 2011), oak shell biowaste (Adibmehr & Faghihian, 2018), sugarcane bagasse (Tao, et al., 2015), hazelnut husks (Imamoglu and Tekir, 2008), bamboo (Liu, et al., 2010) coconut shell (Sekar et al., 2004), date palm fiber (Melliti et al., 2023) Since biomass-derived adsorbents are both cost-effective and efficient, date seeds were chosen for this study due to their widespread availability, low ash content, distinct natural structure, and rich lignocellulosic composition.

However, untreated activated carbon exhibits relatively low adsorption capacity for heavy metals because the functional groups involved in metal binding are only present on a limited portion of its surface. Many materials such as 1,5-diphenylthiocarbazone (Kazemi, et al., 2016), 3-mercaptopropyltrimethoxysil-ane (Xia, et al., 2019), A xanthate (Gao et al., 2017), Eriochrome Blue Black (Albishri et al., 2017), Fe_3O_4 (Arul et al., 2023), EDTA [43], and polyethyleneimine (Saleh, et al., 2017) have been used for the modification of activated carbon to enhancement the adsorption efficiency of metal ions from aqueous media. Lv et al. (2018) enhanced bamboo-activated carbon by modifying it with ethylene diamine tetraacetic acid, creating a novel adsorbent (BAC@SiO2-EDTA) specifically designed for the removal of Pb(II) from water. They found that the adsorption capacity of BAC@SiO_2-EDTA toward Pb(II) (45.45 mg/g) and Cu(II) (23.45 mg/g) was better than raw bamboo activated carbon (Pb(II): 6.85 mg/g, Cu(II): 42.19 mg/g) due to introduced amino groups on the BAC@SiO_2 (Lv et al., 2018). Thiourea is an organosulfur compound with the formula NH_2CSNH_2. Thiourea contains sulfide and nitrogen atoms in its structure, which are used to bind heavy metals (Cai, et al., 2019 and El-Bahy et al., 2003). The introduction of amine and thiol groups on the activated carbon well improves the removal efficiency of lead (II) ions due to their high coordination ability with lead (II) ions.

This study aims to develop a novel, low-cost, and efficient thiourea-modified date seed activated carbon (ACDS@Tu) using a simple method and to evaluate its effectiveness in removing Pb(II) from aqueous solutions. The activated carbon was produced from date seeds through chemical activation

with KOH, followed by modification with thiourea. This resulted in a novel adsorbent with a high Pb(II) ion adsorption capacity. FTIR, XRD, TGA, EDX, SEM, BET, and zeta potential were used to study and characterize the ACDS@Tu composite. The influence of Pb(II) ion concentration, pH value, adsorbent dosage, temperature, and contact time on the Pb(II) removal efficiency was studied. The results revealed that introducing amine and thiol groups on date seed-activated carbon effectively removed Pb(II) ions from the aqueous media. Additionally, the adsorption mechanism of Pb(II) on ACDS@Tu composite was analyzed using kinetic, isotherm, and thermodynamic data.

MATERIALS AND METHODS

1. Materials

Thiourea, Lead nitrate $Pb(NO_3)_2$, anhydrous dichloromethane (DCM), Ethanol (EtOH), and dimethylformamide (DMF) were obtained from Sigma Aldrich. Nitric acid (70%) and Hydrochloric acid (37%) were obtained from Merck, Germany. Sodium hydroxide (98%) was supplied by BDH, England

Instrumentals

The surface morphology of the ACDS and ACDS@Tu composite was investigated using a scanning electron microscope (SEM) from Hitachi Ltd., Tokyo, Japan. The BET of the ACDS and ACDS@Tu composite was measured using a micrometric Tristar II 3020 surface area. The fictional groups of ACDS, ACDS@Tu, and Pb(II) loaded ACDS@Tu composite was determined by FTIR (Thermo Nicolet iS10 spectrometer). A TGA -51 Shimadzu TGA analyser obtained the thermal stability of the ACDS@Tu composite.

Methods

Preparation of ACDS@Tu composite

Preparation of date stones porous activated carbon

The date stones for this study were sourced from Bisha, Saudi Arabia, and underwent a series of preparation steps. Initially, the stones were washed with distilled water, dried in an oven at 100°C for 24 hours, and then ground into a fine powder. A mixture of 20 mg of this powdered date stone and 80 g of KOH (1:4 weight ratio) was created, combined with 100 mL of distilled water, and stirred at 70°C until water evaporation was complete.

This preparation was further dried at 110°C for 24 hours. Following drying, the sample was carbonized in a tubular electric furnace at 400°C for three hours under a nitrogen flow of 75 mL/min. The resulting KOH-activated carbon was treated with 1N HCl, rinsed with warm distilled water to eliminate any acid traces, dried at 110°C for another 24 hours, and finally sieved to 212 µm particle size. This activated carbon was then used for further textural and chemical analyses (Fig. 1).

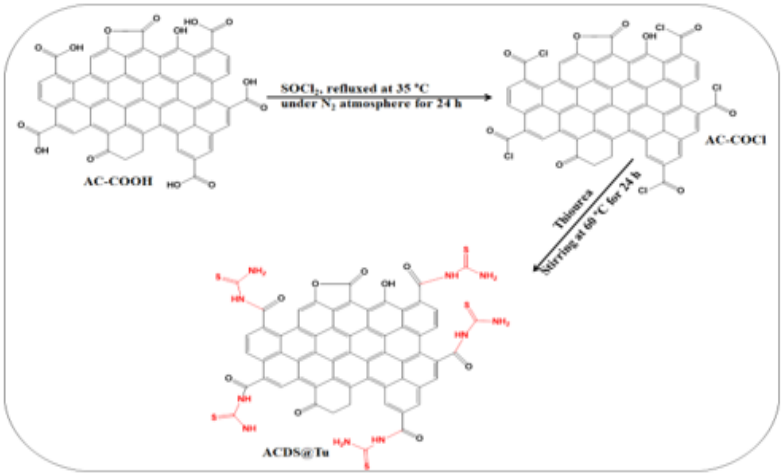

Fig. 1. Scheme illustrate the prepared ACDS@Tu composite.

Synthesis of activated carbon modified thiourea

Porous activated carbon modified thiourea was synthesized according to three steps: in the first step, 4 g of activated carbon was put into 250 mL HNO_3 solution (32.5%) under the magnetic stirring for 24 h. at 60 °C, then the AC-COOH was filtered, washed with D.W., then oven-dried at 80 °C for 24 h. In the second step, 3 g of AC-COOH with 250 mL of a 4:1 mixture of DCM and $SOCl_2$ was refluxed at 35 °C in an N_2 gas for 24 h. The resultant AC-COCl was dried via rotary evaporation at 40° C. Then the AC-COCl was washed with ethanol and D.W. and dried overnight in the oven at 60 °C. In the third step, 2 g of thiourea was dissolved in 50 ml of DMF, and 2 g of AC-COCl was added to the solution. After that, the mixture was stirred at 60 °C for 24 h. The obtained ACDS@Tu was rinsed with acetone and dried in air at 100 °C (Fig. 2).

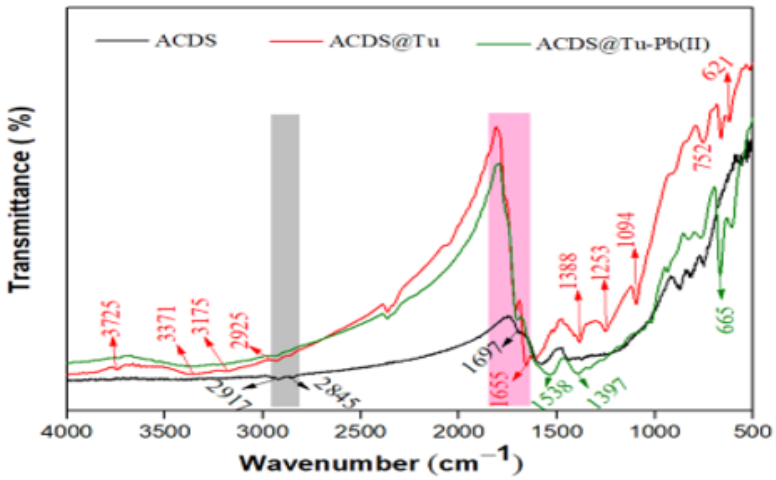

Fig. 2. FTIR spectra of ACDS, ACDS@Tu, and Pb(II) loaded- ACDS@Tu composite.

Batch method adsorption studies

Batch adsorption experiments were carried out to determine the optimal Pb(II) removal conditions using the ACDS@Tu composite. Parameters such as temperature (25–45°C), pH (2–7), adsorbent dose (0.005–0.02 g), initial Pb(II) concentration (50–650 mg/L), and contact time (10–400 min) were varied to assess their effects on adsorption. In each experiment, 50 mL of a Pb(II) solution (50 mg/L) at approximately pH 6 was placed in a 250 mL conical flask and shaken at 100 rpm for 360 minutes at room temperature. Afterward, the ACDS@Tu composite was separated by centrifugation, and the

remaining Pb(II) concentration was measured using ICP-OES. Each test was conducted in triplicate to ensure accuracy, with adsorption capacities calculated from the difference between initial and final concentrations (Eq. 1). The Pb(II) removal efficiency was determined using Eq. 2.

$$q_t = \frac{(C_o - C_e) * V}{m} \quad (1)$$

$$Removal\ (\%) = \frac{C_o - C_e}{C_o} \times 100 \quad (2)$$

In this context qt (mg/g) indicates the quantity of Pb(II) ions adsorbed onto the ACDS@Tu composite at time t, while C_0 and C_e (mg/L) represents the initial and equilibrium concentrations of Pb(II), in the solution respectively. Here, m is the mass of the ACDS@Tu composite (g), and V (L) stands for the volume of the solution (L).

RESULTS

Characterization of ACDS@Tu

The results were tabulated in **Table 1.** Declared the Nonlinear kinetics model parameters for Pb(II) adsorption on ACDS@Tu composite. While, **Table 2.** Nonlinear isotherm model parameters for Pb(II) adsorption on ACDS@Tu composite. **Table 3.** Comparison of Pb(II) adsorption on various activated carbon adsorbents. Fig. 3 shows the morphology of the porous activated carbon (ACDS) and ACDS@Tu composite. The SEM image for ACDS exhibits high porosity with a uniform pores structure (Fig. 3a). After modification of ACDS with Tu, the SEM images show a heterogeneous rough surface with numerous pores of different sizes, confirming the incorporation of thiourea on the activated carbon surface (**Fig. 3b**).

Fig. 4a displays the thermal stability of the ACDS@Tu composite. The TGA curve of the ACDS@Tu composite can be segmented into three distinct stages. The first stage shows an 8% weight loss at ~100 °C, attributed to releasing physically adsorbed water. In the second stage, a weight loss of approximately ~16% was observed between 100 and 350°C, attributed to the thermal degradation of thiourea (Dai et al., 2019). In the third stage, a ~72.7% weight loss occurred between 350 °C and 800 °C due to the devolatilization of hemicellulose, cellulose, and lignin. The TGA curve also shows that the total weight loss for the ACDS@Tu composite was 96.7% in the 33–800°C range.

Table 1. Nonlinear kinetics model parameters for Pb(II) adsorption on ACDS@Tu composite.

C_o (mg/L)	$q_{e,exp.}$ (mg/g)		Pseudo-first-order				Pseudo-second-order				Elovich		
			$q_{e1,cal.}$ (mg/g)	K_1 (1/min)	R^2		$q_{e2,cal.}$ (mg/g)	K_2 (g/mg-min)	R^2		α (mg/g min)	B (mg/g)	R^2
50	95.84		91.42	0.065	0.9534		96.82	0.0011	0.99159		143.06	0.086	0.99448

Table 2. Nonlinear isotherm model parameters for Pb(II) adsorption on ACDS@Tu composite

Temperature (K)	$q_{e,exp.}$ (mg/g)	*Langmuir*				*Freundlich*				*Dubinin-R*		
		q_m, (mg/g)	K_L (L/mg)	R_L	R^2	K_f, (mg/g) $(L/mg)^{1/n}$	n	R^2	q_s, mg/g	K_{D-R} ($mol^2 KJ^{-2}$)	E ($kJ\ mol^{-1}$)	R^2
298 K	493.34	503.27	0.1023	0.164	0.9972	165.37	5.06	0.9269	461.48	18.097	0.166	0.91

Table 3. Comparison of Pb(II) adsorption on various activated carbon adsorbents.

Adsorbent	Prameters Conditions	q_m(mg/g)	Ref.
EDTA-functionalized bamboo activated carbon	pH-5.3, T- 25 °C, time- 24 h, C_o- 50–100 mg/L, dose- 0.8g/L	123.45	[43]
Modified AC from sugarcane bagasse	pH-5, T- 25 °C, time- 120 min, C_o- 200–600 mg/L, dose- 0.1 g	212.13	[65]
Porous activated carbon	pH-5.5, T- 25 °C, time- 120 min, C_o- 25–300 mg/L, dose- 7.5 g/L	207.9	[66]
Amine and thiol modified activated carbon	pH-5.5, T- 25 °C, time- 60 min, C_o- 10–700 mg/L, dose- 0.01 g	310.9	[67]
Polyaniline@activated carbon	pH-4, T- 25 °C, time- 90 min, C_o- 20 mg/L, dose- 1 g	6.81	[68]
Activated carbon derived from date press cake	pH-6, T- 25 °C, time- 45 min, C_o- 5–150 mg/L, dose- 1 g/L	101.3	[69]
ACDS@Tu composite	pH- 6, T- 25 °C, time- 280 min, C_o- 50–650 mg/L, dose- 0.01 g	503.27	This study

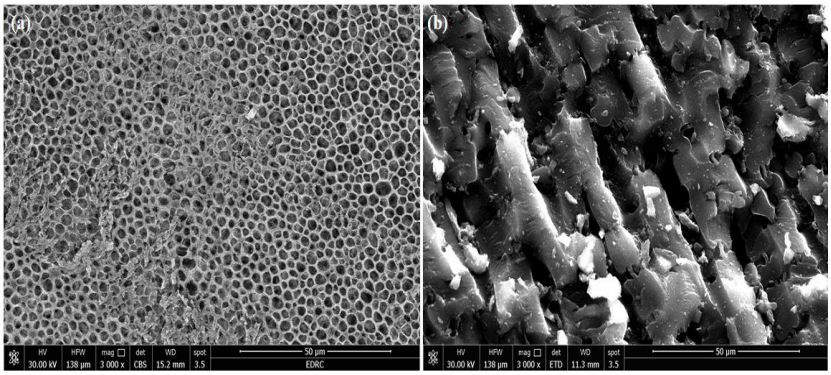

Fig. 3. SEM images of ACDS (a) and ACDS@Tu composite (b).

Fig. 4 b&**c** shows the nitrogen adsorption-desorption isotherms on ACDS and ACDS@Tu composite. The specific surface and total pore volume of ACDS (S_{BET}: 889 m^2/g, V_{tot}: 0.158 cm^3/g) decreased to 155 m^2/g and 0.03 cm^3/g, respectively. This is ascribed to the incorporation of thiourea onto the ACDS surface. The pore radii of ACDS and ACDS@Tu composites were 1.576 and 1.575 nm, respectively. These results confirmed that the pore size of the ACDS and ACDS@Tu composite are consistent with the pore size range of microporous materials (< 2 nm).

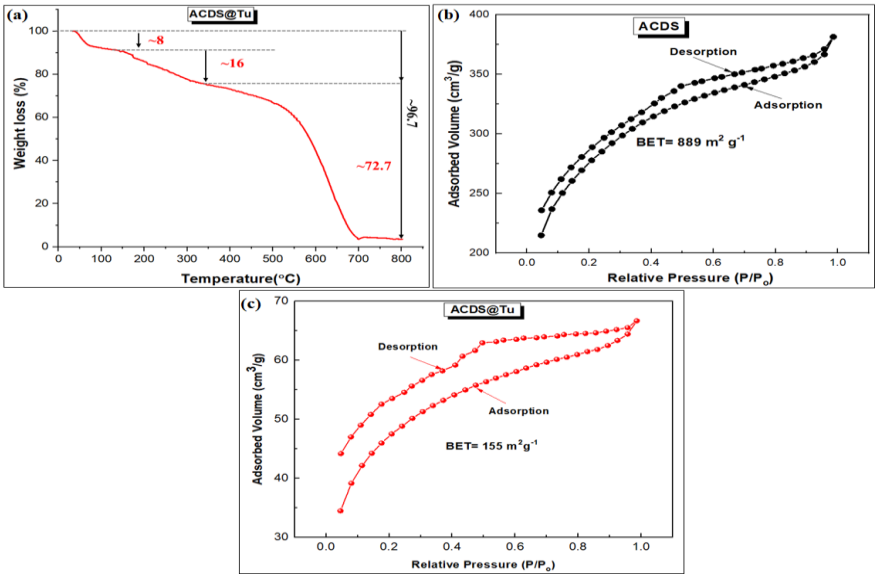

Fig. 4. TGA curve of ACDS@Tu composite (a), N_2 adsorption/desorption isotherms for ACDS (b) and ACDS@Tu composite (b).

Adsorption performance of ACDS@Tu composite

pH Effect

The pH plays is vital in determining the adsorption efficiency of Pb(II) onto the ACDS@Tu composite. As the pH increased from 2 to 6, the adsorption capacity gradually increased, reaching a maximum of 95.84 mg/g at pH 6 (**Fig 5a**). This improvement is due to reduced competition with H^+ ions as the pH becomes more alkaline. However, the adsorption capacity decreased when the pH exceeded 6, likely because Pb(II) precipitates as $Pb(OH)_2$.

Adsorbent dose Effect

The effect of adsorbent mass on Pb(II) ion removal using the ACDS@Tu composite was studied in the range of 0.005 to 0.02 g under constant conditions (T: 298 K, Co: 50 mg/L, agitation speed: 100 rpm, time: 24 h) and the result shown in **Fig 5b**. As the adsorbent dose increased from 0.005 to 0.01 g, the Pb(II) removal efficiency improved from 49.80% to 95.78%. This improvement is attributed to the increased number of available adsorption sites. However, after 0.01 g, further increases in the adsorbent dose led to decreased adsorption capacity because the Pb(II) ions became limited, leaving many adsorption sites unoccupied. Therefore, 0.01 g was selected as the optimal adsorbent dose for this study.

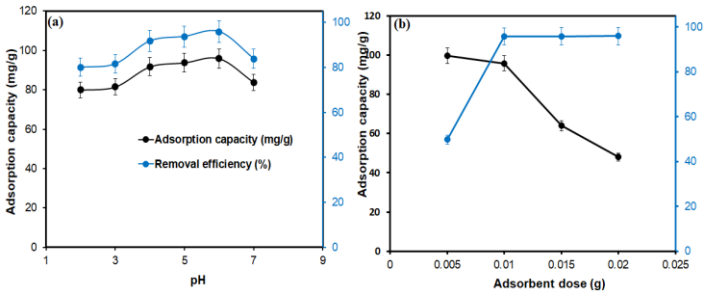

Fig. 5. Influence of initial pH (a) and adsorbent dosage (b) on adsorption of Pb(II) on ACDS@Tu composite.

Contact Time Effect

The influence of contact time on the Pb(II) adsorption on ACDS@Tu composite was investigated from 10 –400 min under the following conditions (C_o: 50 mg/L, pH: 6.0, T: 298 K, *m*: 0.01 g, speed: 100 rpm), as shown in **Fig. 6a**. The results indicated a rapid Pb(II) ions removal within the first 10 min (53.56%), followed by a gradual increase until equilibrium was achieved at 280 min with removal of 95.84%. After 280 min, the adsorption capacity and removal efficiency of Pb(II) levels remained constant. This is because the active adsorption sites on the ACDS@Tu composite are saturated with Pb(II) ions. The highest percentage of removal was 95.84 %. Therefore, an equilibrium time of 280 min was selected for the following experiments.

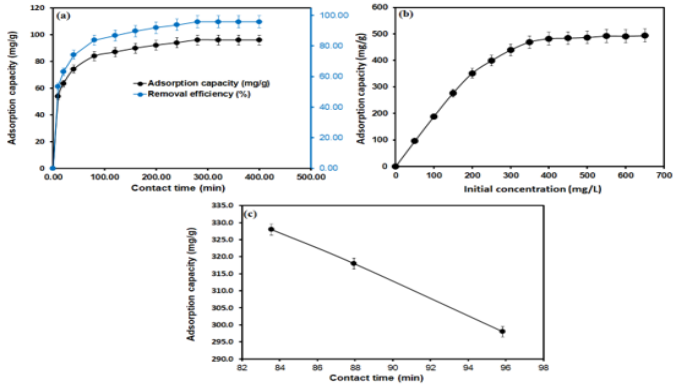

Fig. 6. Influence of contact time (a) and initial concentration (b), and temperature (c) on adsorption of Pb(II) on ACDS@Tu composite

Initial concentration and temperature Effect

The effect of initial Pb(II) concentration on adsorption capacity was examined in the range of 50 to 650 mg/L under the following conditions [(m: 0.01 g, pH: 6.0, T: 298 K, time: 280 min, agitation speed: 100 rpm,), as presented in **Fig. 6b**. The finding revealed that the adsorption capacity of ACDS@Tu composite for Pb(II) ions increased from 85.49 to 439.14 mg/g with increasing amount of Pb(II) from 50 to 300 min. Then, it slightly increases due to the saturation of the adsorption site with Pb(II) ions. The initial increase in capacity with higher Pb(II) concentrations can be attributed to enhanced Pb(II) mass transfer from the solution to the surface of the ACDS@Tu composite. In addition, as the temperature raised from 25°C to 45°C, the amount of Pb(II) adsorbed on ACDS@Tu composite decreased from 95.84 to 83.56 mg/g at 50 mg/L, as shown in **Fig. 6c**, suggesting that the Pb(II) adsorption is exothermic.

Adsorption modeling

Adsorption isotherms

Table 2 provides the isotherm parameters for Pb(II) adsorption on the ACDS@Tu composite, and **Fig. 7b** illustrates the fitting results. Based on the R^2 values in Table 2, the Langmuir model (R^2 = 0.9972) offers a superior fit compared to the Freundlich (R^2 = 0.92698) and Dubinin–Radushkevich (R^2 = 0.91) models, suggesting that the adsorption process on ACDS@Tu composite surfaces is homogeneous and follows a monolayer chemisorption mechanism. The composite's maximum adsorption capacity (qm) was 503.27 mg/g. Additionally, the R_L value in Table 2 indicates favorable Pb(II) adsorption on ACDS@Tu, as it is less than 1.0. This study also compares the adsorption capacity of the ACDS@Tu composite with other adsorbents using the Langmuir isotherm model, as detailed in Table 3. The comparison highlights that the ACDS@Tu composite outperforms other adsorbents like EDTA-functionalized bamboo activated carbon (123.45 mg/g), modified activated carbon from sugarcane bagasse (212.13 mg/g).

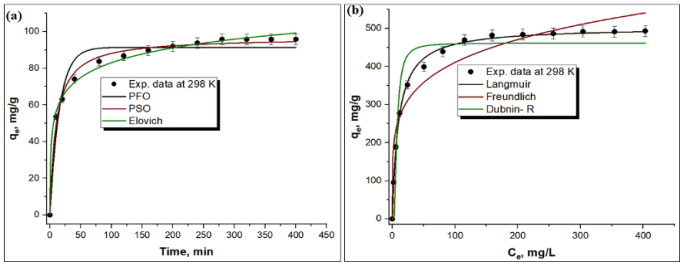

Fig. 7. Isotherm adsorption curves (a) and Kinetic adsorption isotherms (b) of Pb(II) on ACDS@Tu composite.

Adsorption thermodynamics

The plot of ln K_c Vs 1/T is shown in **Fig. 8**, and **Table 4** summarizes the thermodynamic values for Pb(II) adsorption on the ACDS@Tu composite.

Table 3. Thermodynamic parameters for Pb(II) adsorption on ACDS@Tu composite

Concentration	ΔH° (kJ/mol)	ΔS° (J/mol.K)	(-)ΔG° (kJ/mol)		
			294 K	298 K	303 K
50	-3.67	-6.88	-1.62	-1.49	-1.41

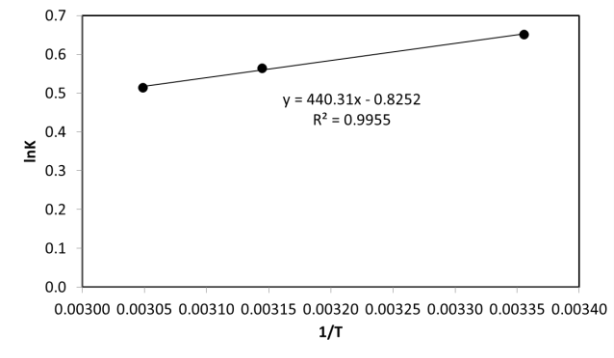

Fig. 8. Plot of lnK vs. 1/T for thermodynamic parameters calculation

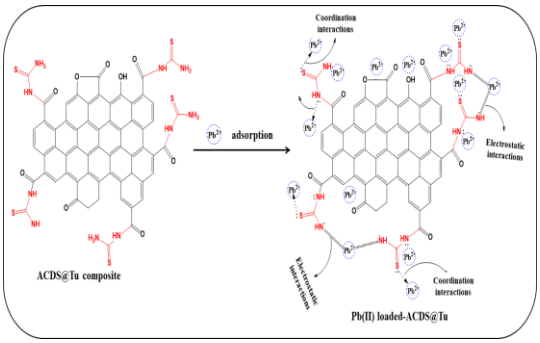

Fig. 9. Mechanism adsorption of Pb

DISCUSSION

The FTIR spectra of ACDS, ACDS@Tu, and Pb(II)-loaded ACDS@Tu (Fig. 2) reveal significant differences in surface functional groups. In ACDS, characteristic peaks were detected at 2917 and 2845 cm–1 for C–H stretching (asymmetry and symmetry), 1707 cm^{-1} for C=O stretching, 1582 cm^{-1} for C=C in the aromatic ring, and 1442 cm^{-1} for aliphatic C–H bending, indicating the presence of lignocellulosic components and functional groups such as alcohols, ketones, aldehydes, and aromatic compounds (Elnour, et al., 2019).Upon modification with thiourea, new peaks appeared in ACDS@Tu at 3175 and 3371 cm–1, associated with NH_2 overlapping with OH, and at 1655 cm^{-1}, corresponding to the amide (–CONH) stretching. Additionally, peaks at 752 and 620 cm^{-1} indicated C=S asymmetric and symmetric stretching, confirming successful thiourea incorporation (Singh et al., 2020). The peak at 1615 cm–1 is attributed to NH bending (Naushad et al., 2019 and Melhi et al., 2024) and peaks at 1383, 1251, and 1094 cm^{-1} are linked to C–O and C–N stretching (Mariappan et al., 2011). Several characteristic bonds diminished or disappeared after Pb(II) adsorption, suggesting Pb(II) binding. The 3175 and 3371 cm^{-1} peaks for NH/OH stretching showed reduced intensity. Additionally, peaks at 1655 and 1615 cm^{-1}, related to amide and NH_2 bending, decreased and shifted to 1538 cm^{-1}, indicating electrostatic interactions between Pb(II) and the amino and hydroxyl groups of ACDS@Tu. The disappearance of C=S, C–O, and C–N bands after Pb(II) adsorption confirms that -NH_2, -CONH, and -OH groups in ACDS@Tu actively participate in Pb(II) uptake

The first stage shows an 8% weight loss at ~100 °C, attributed to the release of physically adsorbed water. In the second stage, a weight loss of approximately ~16% was observed between 100 and 350°C, attributed to the thermal degradation of thiourea (Dai et al., 2019). In the third stage, a ~72.7% weight loss occurred between 350 °C and 800 °C due to the devolatilization of hemicellulose,

cellulose, and lignin. The TGA curve also shows that the total weight loss for the ACDS@Tu composite was 96.7% in the 33–800°C range.

The improvement is due to reduced competition with H^+ ions as the pH becomes more alkaline. However, the adsorption capacity decreased when the pH exceeded 6, likely because Pb(II) precipitates as $Pb(OH)_2$. As a result, pH 6 was chosen as the optimal condition for the subsequent experiments. Similar findings were observed in the removal of Pb(II) using pine cone adsorbents (Xu et al., 2021 and Fu et al, 2019). A similar result was observed for the influence of pH on the elimination of Pb(II) on pine cone (Selvi and Balasubramaniyan, 2024).

The effect of initial Pb(II) concentration on adsorption capacity was examined in the range of 50 to 650 mg/L under the following conditions [(m: 0.01 g, pH: 6.0, T: 298 K, time: 280 min, agitation speed: 100 rpm,), as presented in **Fig. 6b**. The finding revealed that the adsorption capacity of ACDS@Tu composite for Pb(II) ions increased from 85.49 to 439.14 mg/g with increasing amount of Pb(II) from 50 to 300 min. Then, it slightly increases due to the saturation of the adsorption site with Pb(II) ions. The initial increase in capacity with higher Pb(II) concentrations can be attributed to enhanced Pb(II) mass transfer from the solution to the surface of the ACDS@Tu composite. In addition, as the temperature raised from 25°C to 45°C, the amount of Pb(II) adsorbed on ACDS@Tu composite decreased from 95.84 to 83.56 mg/g at 50 mg/L, as shown in **Fig. 6c**, suggesting that the Pb(II) adsorption is exothermic. The decrease in adsorption capacity may be due to weak attraction between Pb(II) ions and ACDS@Tu composite at higher temperatures. Similar trends were reported by Bilal et al., (2021) for the adsorption of Pb(II) on activated carbon and activated carbon mesoporous adsorbent (Neolak et al. 2021), respectively.

To investigate the adsorption kinetics mechanisms for Pb(II) on the ACDS@Tu composite, three kinetic models were analyzed: the pseudo-first-order (PFO) model (Lagergren, 1898), the pseudo-second-order (PSO) model (Wingenfelder et al., 2005), and the Elovich model (George, and Roginsky, 1934). The nonlinear equations for these models are provided in the supplementary material (Text S1). Table 1 presents the kinetic parameters for Pb(II) adsorption on the ACDS@Tu composite, while the fitting results are shown in Fig. 7a. Findings indicate that the PSO and Elovich models better predict Pb(II) adsorption on the ACDS@Tu composite, achieving higher R^2 values of 0.99159 compared to the PFO model (R^2 = 0.9534). Additionally, the calculated $q_{e,cal}$ (96.82 mg/g) by PSO agree with experimental values ($q_{e,exp}$) (95.84 mg/g), suggesting that Pb(II) adsorption involves chemical adsorption via electron sharing between the ACDS@Tu composite and Pb(II) ions (Yin, et al., 2019). Similar observations for Pb(II) removal have been reported by Bilal et al. using activated carbon.

To explore the mechanisms of Pb(II) adsorption on the ACDS@Tu composite, three isotherm models—Langmuir (Wallis & Dollard, 2008), Freundlich, and Dubinin–Radushkevich (Dubinin, 1947) were applied. The equations for these isotherm models are available in the supplementary material (Text S2). The composite's maximum adsorption capacity (qm) was 503.27 mg/g. Additionally, the R_L value in Table 2 indicates favorable Pb(II) adsorption on ACDS@Tu, as it is less than 1.0. This study also compares the adsorption capacity of the ACDS@Tu composite with other adsorbents using the Langmuir isotherm model, as detailed in Table 3. The comparison highlights that the ACDS@Tu composite outperforms other adsorbents like EDTA-functionalized bamboo activated carbon (123.45 mg/g) (Liu et al., 2018), modified activated carbon from sugarcane bagasse (212.13 mg/g) (Somyanonthanakun et al., 2023), porous carbon (207.9 mg/g) (El-Wakeel, et al., 2023), AT-MAC (310.9 mg/g) (Waly et al., 2021), Polyaniline@activated carbon (6.81 mg/g) [68], and activated carbon derived from date press cake (101.3 mg/g) (Heidarinejad et al., 2019). These findings underscore the ACDS@Tu composite's high efficiency in removing Pb(II) from aqueous environments.

To assess the feasibility and spontaneity of Pb(II) adsorption onto the ACDS@Tu composite, thermodynamic parameters—entropy (ΔS° in J/mol/K), Gibbs free energy (ΔG° in kJ/mol), and enthalpy (ΔH° in kJ/mol) were calculated using the equations provided below. The values for enthalpy and entropy were obtained from the slope and intercept of the van't Hoff plot, respectively.

$$lnK_c = -\frac{\Delta H^0}{RT} + \frac{\Delta S^0}{R}$$

$$\Delta G° = -RT\ lnKc$$

where K_c represents the thermodynamic equilibrium constant, defined as the ratio of qe to Ce. The plot of ln K_c Vs 1/T is shown in **Fig. 8**, and **Table 4** summarizes the thermodynamic values for Pb(II) adsorption on the ACDS@Tu composite. The negative enthalpy value (-3.67 kJ/mol) indicates that the removal of Pb(II) on the composite surface is an exothermic process, suggesting a physical adsorption mechanism (physisorption) (Shi et al., 2021). The negative ΔG° values (−1.62 and −1.41 kJ/mol) demonstrate that Pb(II) adsorption on the ACDS@Tu composite is spontaneous. Furthermore, as the ΔG° values decrease with rising temperature from 298 to 328 K, it is evident that lower temperatures (298 K) enhance Pb(II) adsorption on the composite. The negative ΔS° value (−6.88 J/mol.K) reflects a reduction in disorder at the solid-liquid interface. Similar trends in Pb(II) removal have been reported by Alqadami et al. (2020[a]) with silico-manganese fume-impregnated cryogenic alginate beads (Alqadami et al., 2020[b] and Alsuhybani et al. (2020) using Fe3O4@BDC@AGPA.

CONCLUSION

Thiourea-modified activated carbon derived from date stones (ACDS@Tu) was synthesized and demonstrated remarkable efficiency in adsorbing Pb(II) ions from water. FTIR analysis confirmed the successful incorporation of thiourea onto the activated carbon framework through an amidation reaction. ACDS@Tu exhibited a specific surface area of 889 m^2/g and a pore volume of 0.158 cm^3/g. Investigations revealed that factors such as contact time, temperature, pH, initial Pb(II) concentration, and adsorbent dosage all positively impacted adsorption performance. Under optimal conditions (pH 6.0, Pb(II) concentration of 50 mg/L, temperature of 298 K, adsorbent dose of 0.01 g, and agitation at 100 rpm), Pb(II) removal reached 95.84%. The adsorption kinetics followed the PSO model, and equilibrium data conformed to the Langmuir isotherm, indicating a maximum adsorption capacity of 503.27 mg/g. Thermodynamic studies showed the process to be exothermic. The adsorption mechanism primarily involved electrostatic interactions and minimal chemisorption, making ACDS@Tu a cost-effective, sustainable, and highly effective adsorbent for Pb(II) removal from water and wastewater.

AUTHORS' CONTRIBUTIONS

ASA: the researcher who performed all tests and wrote the research draft and data analysis; BJ wrote the study's design. NTE: The manuscript's correspondent author made edits to the paper. RFH: made edits to the paper. AAN: made edits to the paper. All writers read and approved the final manuscript.

ACKNOWLEDGMENT

The authors declare no financial support

DECLARATION OF COMPETING INTEREST

There are no conflicts to declare.

REFERENCES

Ahamad TM, Naushad SM, Alshehri AM, 2020. Fabrication of magnetic polymeric resin for the removal of toxic metals from aqueous medium: Kinetics and adsorption mechanisms, J Water Process Eng. 36: 101-128.

Algethami JS, Alqadami AA, Melhi SM, Alhamami MA, Fallatah AM, Rizk MA, 2022. Sulfhydryl Functionalized Magnetic Chitosan as an Efficient Adsorbent for High-Performance Removal of Cd(II) from Water: Adsorption Isotherms, Kinetic, and Reusability Studies, Adsorpt Sci Technol. 22: 48-55.

Algamdi MS, Alghamdi AS, Alsohaimi IH, Allohybi FD, Alqadami AA, 2017. Preconcentration of heavy metals on multiwalled carbon nanotubes in water samples prior to analysis using FAAS, Desalin Water Treat. 69: 15-25.

Alqadami AA, Khan MA, Siddiqui MR, Alothman ZA, Sumbul SA, 2020[b]. A facile approach to develop industrial waste encapsulated cryogenic alginate beads to sequester toxic bivalent heavy metals, J King Saud Univ - Sci. 32: 42-50.

Alqadami AA, Naushad MA, ALOthman ZA, Alsuhybani MS, Algamdi MA, 2020[a]. Excellent adsorptive performance of a new nanocomposite for removal of toxic Pb(II) from aqueous environment: Adsorption mechanism and modeling analysis, J Hazard Mater. 389: 12-18.

Alqadami AA, Naushad MA, Abdalla MA, Khan MR, Alothman ZA, Wabaidur SM, Ghfar AA, 2017. Determination of heavy metals in skin-whitening cosmetics using microwave digestion and inductively coupled plasma atomic emission spectrometry, IET Nanobiotechnology. 11: 17-25.

Alqadami MA, Naushad Mu, Ahamad TA, Alshahrani AA, Usluc HA, Shukla SK, 2020 Alqadami et al., 2020[b]. Removal of highly toxic Cd(II) metal ions from aqueous medium using magnetic nanocomposite: adsorption kinetics, isotherm and thermodynamics, Desalin Water Treat. 181: 355–361.

Adibmehr MS, Faghihian HA, 2018. Magnetization and functionalization of activated carbon prepared by oak shell biowaste for removal of Pb2+ from aqueous solutions, Chem Eng Commun. 205: 519–532.

Aldawsari AA, Khan MA, Hameed BH, Alqadami AA, Siddiqui MR, Alothman ZA, Ahmed AH, 2017. Mercerized mesoporous date pit activated carbon - A novel adsorbent to sequester potentially toxic divalent heavy metals from water, PLoS One. 12: 1–17.

Algethami JS, Alhamami MA, Alqadami AA, Melhi SM, Seliem AF, 2024. Magnetic hydrochar grafted-chitosan for enhanced efficient adsorption of malachite green dye from aqueous solutions: Modeling, adsorption behavior, and mechanism analysis, Int J Biol Macromol. 254: 12-17.

Aldawsari AM, Alsohaimi IH, Al-Kahtani AA, Alqadami AA, Ali ZE, Saleh EM, 2021. Adsorptive performance of aminoterephthalic acid modified oxidized activated carbon for malachite green dye: mechanism, kinetic and thermodynamic studies, Sep Sci Technol. 56: 835–846.

Alsuhybani MA, Alshahrani MA, Algamdi AA, 2020. Al-Kahtani, A.A. Alqadami, Highly efficient removal of Pb(II) from aqueous systems using a new nanocomposite: Adsorption, isotherm, kinetic and mechanism studies, J Mol Liq. 301: 11-23.

Albishri HM, Marwani MG, Batterjee EM, Soliman HM, 2017. Eriochrome Blue Black modified activated carbon as solid phase extractor for removal of Pb(II) ions from water samples, Arab J Chem. 10: S1955–S1962.

Arul AM, Kavitha SA, Anand BC, Surya A, Ravikumar Y, Sivalingam HA, 2023. Enhanced removal of Pb (II) and Cd (II) ions from aqueous systems using coated magnetic nanoparticles in activated carbon derived from corncob waste, Surfaces and Interfaces. 40: 10-15.

Bilal MA, Ali MY, Khan RJ, Uddin FA, Kanwl AM, 2021. Synthesis and characterization of activated carbon from Capparis decidua for removal of Pb(II) from model aqueous solution: kinetic and thermodynamics approach, Desalin Water Treat. 221: 185–196.

Burke DM, Morris JD, Holmes MA, 2013. Chemical oxidation of mesoporous carbon foams for lead ion adsorption, Sep Purif Technol. 104: 150–159.

Cai WA, Zhu HF, Liang YA, Jiang WM, Tu ZC, Cai JA, Wu JV, Zhou AS, 2019. Preparation of thiourea-modified magnetic chitosan composite with efficient removal efficiency for Cr(VI), Chem Eng Res Des. 144: 150–158.

Dai AC, Zhang HA, Li RA, Zou HM, 2019. Synthesis and characterization of thiourea, Polish J Chem Technol. 21: 35–39.

Di Palma LA, Ferrantelli PO, Merli CA, Petrucci EA, 2002. Treatment of industrial landfill leachate by means of evaporation and reverse osmosis, Waste Manag. 22: 951–955.

Dubinin LV, 1947. Equation of the characteristic curve of activated charcoal, Proc Acad Sci USSR, Phys Chem Sect. 1: 857-62.

El-Bahy GM, El-Sayed AA, Shabana BA, 2003. Vibrational and electronic studies on some metal thiourea complexes, Vib Spectrosc. 31: 101–107.

Elnour AY, Alghyamah AA, Shaikh HM, Poulose AM, Al-Zahrani SM, Anis A, Al-Wabel MI, 2019. Effect of Pyrolysis Temperature on Biochar Microstructural Evolution, Physicochemical Characteristics, and Its Influence on Biochar/Polypropylene Composites, Appl Sci. 9:15-24

El-Wakeel ST, Fathy NA, Tawfik ME, 2023. Porous carbons prepared from a novel hard wood composite waste for effective adsorption of Pb(ii) and Cd(ii) ions, RSC Adv. 13: 34935-46.

Fu L, Wang SA, Lin LG, Zhang QM, Liu HN, Zhou AC, Kang SG, Wan HA, Li SL, 2019. Wen, Post-modification of UiO-66-NH2 by resorcyl aldehyde for selective removal of Pb(II) in aqueous media, J Clean Prod. 229: 470–479.

Gao TA, Yu JN, Zhou YX, JiangAM, 2017. Performance of xanthate-modified multi-walled carbon nanotubes on adsorption of lead ions, Water, Air, Soil Pollut. 228: 1–12.

Ghasemi MM, Naushad NA, Ghasemi YS, Khosravi-fard AM, 2014. Adsorption of Pb(II) from aqueous solution using new adsorbents prepared from agricultural waste: Adsorption isotherm and kinetic studies, J Ind Eng Chem. 20: 2193–2199.

George SA, and Roginsky BZ, 1934. The catalytic oxidation of carbon monoxide on manganese dioxide, Acta Phys Chem USSR. 1: 554-560.

Heidarinejad ZA, Rahmanian OM, Heidari AN, 2019. Production of KOH-activated carbon from date press cake: effect of the activating agent on its properties and Pb(II) adsorption potential, Desalin Water Treat. 165: 232–243.

Imamoglu AM, Tekir MO, 2008. Removal of copper (II) and lead (II) ions from aqueous solutions by adsorption on activated carbon from a new precursor hazelnut husks, Desalination. 228: 108–113.

Kariri MA, Alsohaimi IM, Alzaid MS, Alhumaimess AA, Alqadami MY, El-Sayed AM, Aldawsari SH, Mohamed HM, Hassan IH, 2024. Transformative strategies for heavy metals extraction: Ionic liquid-boosted fizzy capsule for distributive solid-phase microextraction in aquatic environments, J Ind Eng Chem. 3(5): 11-21 .

Kazemi AF, Younesi AA, Ghoreyshi HN, Bahramifar AM, Heidari GA, 2016. Thiol-incorporated activated carbon derived from fir wood sawdust as an efficient adsorbent for the removal of mercury ion: Batch and fixed-bed column studies, Process Saf Environ Prot. 100: 22–35.

Khan MA, Alqadami SM, Wabaidur BA, Jeon AA, 2023. Co-Carbonized Waste Polythene/Sugarcane Bagasse Nanocomposite for Aqueous Environmental Remediation Applications, Nanomaterials. 13: 23-33.

Khan MA, Alqadami MA, Otero AA, Siddiqui MR, Alothman ZA, Alsohaimi IM, Rafatullah AE, Hamedelniel MN, 2019[a]. Heteroatom-doped magnetic hydrochar to remove post-transition

and transition metals from water: Synthesis, characterization, and adsorption studies, Chemosphere. 218: 1089–1099.

Lagergren SA, 1898. About the theory of so-called adsorption of soluble substances, Handlingar. 24: 1–39.

Liu QS, Zheng PT, Wang LM, Guo AM, 2010. Preparation and characterization of activated carbon from bamboo by microwave-induced phosphoric acid activation, Ind Crops Prod. 31: 233–238.

Lv DM, Liu YA, Zhou JK, Yang ZM, Lou SA, Baig XA. Xu MA, 2018. Application of EDTA-functionalized bamboo activated carbon (BAC) for Pb(II) and Cu(II) removal from aqueous solutions, Appl Surf Sci. 428: 648–658.

Lee LS, Lingamdinne, JK, Yang JR, Koduru YY, Chang MA, Naushad LP, 2022. Biopolymer mixture-entrapped modified graphene oxide for sustainable treatment of heavy metal contaminated real surface water, J Water Process Eng. 46: 10-26.

Mariappan MA, Madhurambal BG, Ravindran SC, Mojumdar AM, 2011. Thermal, FTIR and microhardness studies of bisthiourea-urea single crystal, J Therm Anal Calorim. 104: 915–921.

Majdoubi HA, Alqadami RE, Billah MA, Otero BH, Jeon HA, Hannache AM, Tamraoui MA, Khan AA, 2023. Chitin-Based Magnesium Oxide Biocomposite for the Removal of Methyl Orange from Water, Int J Environ Res Public Health. 20: 23-29.

Maneechakr PA, Karnjanakom SA, 2021. Facile utilization of magnetic MnO2@Fe3O4@sulfonated carbon sphere for selective removal of hazardous Pb(II) ion with an excellent capacity: Adsorption behavior/isotherm/kinetic/thermodynamic studies, J Environ Chem Eng. 9: 10-16.

Matlock MM, Howerton DA, Atwood BS, 2002. Chemical precipitation of heavy metals from acid mine drainage, Water Res. 36: 4757–4764.

Melhi MS, Algamdi AA, Alqadami MA, Khan EH, Alosaimi AM, 2022. Fabrication of magnetically recyclable nanocomposite as an effective adsorbent for the removal of malachite green from water, Chem Eng Res Des. 177: 843–854.

Melhi SA, Alqadami EH, Alosaimi GM, Ibrahim BA, El-Gammal MA, Bedair EM, Elnaggar AA, 2024. Effective Removal of Malachite Green Dye from Water Using Low-Cost Porous Organic Polymers: Adsorption Kinetics, Isotherms, and Reusability Studies, Water. 16: 29-35.

Melhi SA, 2022. Novel carbazole-based porous organic frameworks (CzBPOF) for efficient removal of toxic Pb(II) from water: Synthesis, characterization, and adsorption studies, Environ Technol Innov. 25: 10-21.

Melliti MA, Yılmaz MM, Sillanpää BA, Hamrouni RA, Vurm MG, 2023. Low-cost date palm fiber activated carbon for effective and fast heavy metal adsorption from water: Characterization, equilibrium, and kinetics studies, Colloids Surfaces A Physicochem Eng Asp. 672: 13-17.

Momčilović MM, Purenović AM, Bojić AM, Zarubica MG, Ranđelović SA, 2011. Removal of lead(II) ions from aqueous solutions by adsorption onto pine cone activated carbon, Desalination. 276: 53–59.

Naushad MA, Alqadami, AT, Ahamad AA, 2020. Removal of Cd(II) ion from aqueous environment using triaminotriethoxysilane grafted oxidized activated carbon synthesized via activation and subsequent silanization, Environ Technol Innov. 18: 100-108.

Naushad MA, Alqadami ZA, AlOthman IH, Alsohaimi MS, Algamdi AM, Aldawsari NG, 2019. Adsorption kinetics, isotherm and reusability studies for the removal of cationic dye from aqueous medium using arginine modified activated carbon, J Mol Liq. 293: 11-14.

Naushad MA, Khan ZA, ALOthman AH, Al-Muhtaseb MR, Awual AA, Alqadami MR, 2020. Water Purification Using Cost Effective Material Prepared from Agricultural Waste: Kinetics, Isotherms, and Thermodynamic Studies, Clean - Soil, Air, Water. 44: 16-25.

Naushad MA, 2014. Surfactant assisted nano-composite cation exchanger: Development, characterization and applications for the removal of toxic Pb2+ from aqueous medium, Chem Eng J. 235: 100–108.

Tao HC, Zhang JB, Li WY, Ding HR, 2015. Biomass based activated carbon obtained from sludge and sugarcane bagasse for removing lead ion from wastewater, Bioresour Technol. 192: 611–617.

Saad MA, Saeed IS, Hotan AM, 2017. Preconcentration of heavy metals on multiwalled carbon nanotubes in water samples prior to analysis using FAAS, 0426: 1–7.

Saleh TA, Sarı MA, Tuzen SA, 2017. Optimization of parameters with experimental design for the adsorption of mercury using polyethylenimine modified-activated carbon, J Environ Chem Eng. 5: 1079–1088.

Sekar AM, Sakthi AS, Rengaraj GV, 2004. Kinetics and equilibrium adsorption study of lead(II) onto activated carbon prepared from coconut shell, J Colloid Interface Sci. 279: 307–313.

Selvi MS, Balasubramaniyan AN, 2024. Efficient removal of Pb (II) ions from aqueous solution by the Moringa oleifera synthesized magnetic ZnFe2O4 spinel nanoparticles, Desalin Water Treat. 319: 100-105.

Shi, SC, Xu AM, Dong YQ, Wang SM, Zhu XA, Zhang YM, Tak Chow XA, Wang LZ, Zhu GA, Zhang DM, XuSG, 2021. High saturation magnetization MnO2/PDA/Fe3O4 fibers for efficient Pb(II) adsorption and rapid magnetic separation, Appl Surf Sci. 541: 14-18.

Singh AA, Guleria MA, Neogy MC, Rath SA, 2020. UV induced synthesis of starch capped CdSe quantum dots: Functionalization with thiourea and application in sensing heavy metals ions in aqueous solution, Arab J Chem. 13: 3149–3158.

Somyanonthanakun WM, Ahmed VR, Krongtong SS, 2023. Thongmee, Studies on the adsorption of Pb(II) from aqueous solutions using sugarcane bagasse-based modified activated carbon with nitric acid: Kinetic, isotherm and desorption, Chem Phys Impact. 6: 100-108.

Wang NA, Xu AX, Li JH, Zhai LL, Yuan KM, Zhang HA, Yu SA, 2016. Preparation and Application of a Xanthate-Modified Thiourea Chitosan Sponge for the Removal of Pb(II) from Aqueous Solutions, Ind Eng Chem Res. 55: 4960–4968.

Wallis AA, and Dollard MF, 2008. Local and global factors in work stress - The Australian dairy farming examplar, Scand J Work Environ Heal Suppl. 8: 66–74.

Waly SM, El-Wakil WM, El-Maaty FS, Awad AM, 2021. Efficient removal of Pb(II) and Hg(II) ions from aqueous solution by amine and thiol modified activated carbon, J Saudi Chem Soc. 25: 10-29.

Wingenfelder UA, Hansen GC, Furrer RA, 2005. Schulin, Removal of Heavy Metals from Mine Waters by Natural Zeolites, Environ Sci Technol. 39: 4606–4613.

Xia AS, Huang YJ, Tang ML, Wang SA, 2019. Preparation of various thiol-functionalized carbon-based materials for enhanced removal of mercury from aqueous solution, Environ Sci Pollut Res. 26: 8709–8720.

Xu GR, An KM, Xu QA, Liu RS, Das HL, Zhao ZH, 2021. Metal organic framework (MOF)-based micro/nanoscaled materials for heavy metal ions removal: The cutting-edge study on designs, synthesis, and applications, Coord Chem Rev. 427: 21-33.

Yin X., P. Shao, L. Ding, Y. Xi, K. Zhang, L. Yang, H. Shi, X. Luo, Protonation of rhodanine polymers for enhancing the capture and recovery of Ag+ from highly acidic wastewater, Environ Sci Nano. 6 (2019) 3307–3315. https://doi.org/10.1039/C9EN00833K.

Zhu WA, Li DX, Wu JA, Yu YA, Zhou YZ, Luo KA, Wei WA, Ma ZY, 2016. Synthesis of spherical mesoporous silica materials by pseudomorphic transformation of silica fume and its Pb2+ removal properties, Microporous Mesoporous Mater. 222: 192–201.